Strong-coupling solver for the quantum impurity model

Xi Dai,[1,*] Kristjan Haule,[2] and Gabriel Kotliar[3]
[1]*Department of Physics, University of Hong Kong, Hong Kong, China*
[2]*Jožef Stefan Institute, SI-1000 Ljubljana, Slovenia*
[3]*Department of Physics and Center for Material Theory, Rutgers University, Piscataway, New Jersey 08854, USA*
(Received 18 December 2004; revised manuscript received 19 April 2005; published 8 July 2005)

We propose a fast impurity solver for the general quantum impurity model based on the perturbation theory around the atomic limit, which can be used in combination with the local density approximation (LDA) and the dynamical mean-field theory (DMFT). We benchmark the solver in the two-band Hubbard model within DMFT against quantum Monte Carlo (QMC) and numerical renormalization-group (NRG) results. We find that the solver works very well in the paramagnetic Mott insulator phase. We also apply this impurity solver to the DMFT study of the antiferromagnetic phase transition in the unfrustrated Bethe lattice. The Neel temperature obtained by the fast impurity solver agrees very well with the QMC results in the large Hubbard U limit. The method is a promising tool to be used in combination with the LDA+DMFT to study Mott insulators starting from first principles.

DOI: 10.1103/PhysRevB.72.045111 PACS number(s): 71.10.Fd, 71.20.Be

I. INTRODUCTION

Recently, much effort has been devoted to developing methods for *ab initio* investigations of real materials with strongly correlated electrons. A most promising tool was built by combining the conventional first principle methods, such as the density functional theory in the local density approximation (LDA), with the newly developed dynamical mean-field theory (DMFT).[1] Many numerical schemes such as LDA+DMFT,[2] LDA++,[3] *GW*+DMFT[4] have been proposed and applied to various systems.[5,6]

The application of DMFT to real material requires a fast scheme to solve the generalized Anderson impurity model. Many of the impurity solvers, such as the iterative perturbation theory (IPT),[7,8] the noncrossing approximation (NCA),[9] the slave boson mean field,[10] the equation of motion method,[11] the exact diagonalization-based methods,[12] and quantum Monte Carlo (QMC) methods,[13] have been developed for simplified multiorbital Anderson models, usually assuming SU(N) symmetry. Very few tools are available for the study of general Anderson impurity models generated by realistic DMFT calculations. Therefore it is important to develop impurity solvers which can be used for a very general case. In the weak-coupling limit when the system is in the metallic phase, the fluctuation exchange approximation[14] (FLEX) has been proposed and implemented. On the other hand, for the Mott insulator phase when the local interaction term is very strong, we still lack a general impurity solver which can treat models without SU(N) symmetry and contain general crystal fields and multiplet terms. Recent studies on the Mott insulators,[15] i.e., $LaMnO_3$, V_2O_3, $LaTiO_3$, and $YTiO_3$,[16] discovered a variety of phenomena, including orbital order-disorder transition, charge-density wave, and antiferromagnetism. Therefore the first-principles study on the Mott insulator material with or without long-ranger order becomes a very important issue for both the theoretical understanding of these materials and the material designing of these types of compounds.

II. DERIVATION OF THE METHOD

In this paper, we propose an impurity solver which is based on the perturbation theory around the atomic limit. We shall consider the most general Anderson impurity model generated by the LDA+DMFT calculation

$$H_{total} = H_{local} + H_{band} + + H_v, \tag{1}$$

$$H_{local} = \sum_{\alpha\beta} t_{\alpha\beta} f_\alpha^\dagger f_\beta + \frac{1}{2} \sum_{\alpha\beta\gamma\delta} U_{\alpha\beta\gamma\delta} f_\alpha^\dagger f_\beta^\dagger f_\delta f_\gamma, \tag{2}$$

$$H_{band} = \sum_{k\alpha} \epsilon_{k\alpha} c_{k\alpha}^\dagger c_{k\alpha}, \tag{3}$$

$$H_v = \sum_{k\alpha\beta} V_{k\alpha\beta} f_\alpha^\dagger c_{k\beta} + \text{H.c.}, \tag{4}$$

where H_{local} is a very general atomic Hamiltonian and index α denotes the spin and orbital degree of freedom. Further, H_{band} stands for the conducting band which plays the role of a fermionic bath in DMFT calculations.

Our first step is to diagonalize the atomic Hamiltonian H_{local} by the exact diagonalization

$$H_{local} = \sum_m E_m |m\rangle\langle m|, \tag{5}$$

which can be done for any atom on modern computers. The hybridization term then takes the form

$$H_v = \sum_{k\alpha\beta} V_{k\alpha\beta} (F^{\alpha\dagger})_{mm'} |m\rangle\langle m'| c_{k\beta} + \text{H.c.}, \tag{6}$$

where $(F^\alpha)_{mm'} = \langle m|f_\alpha|m'\rangle$ are the matrix elements of the operator f_α in the local eigenbase. The atomic Green's function can be expressed by the eigenstates in the following way:

$$G_{\alpha\beta}^{(atom)}(i\omega) = -\int_0^\beta e^{i\omega\tau}\langle T_\tau f_\alpha(\tau) f_\beta^\dagger(0)\rangle d\tau = \sum_{mm'} \frac{(F^\alpha)_{mm'}(F^{\beta\dagger})_{m'm}(X_m + X_{m'})}{i\omega - E_{m'} + E_m}, \quad (7)$$

where $X_m = e^{-\beta E_m}/Z$ is the probability for the atomic state $|m\rangle$. The atomic self-energy can then be obtained by the inversion of a matrix

$$\Sigma^{(atom)}(i\omega) = (i\omega + \mu - \hat{t})^{-1} - G^{(atom)}(i\omega)^{-1}. \quad (8)$$

This is the zeroth-order self-energy in the expansion around the atomic limit. If we are able to compute the expansion of the Green's function in powers of the hybridization, i.e., $G = G^{(atom)} + G^{(2)} + O(V^4)$, we could also express the correction to the self-energy using the Dyson equation

$$G = (i\omega + \mu - \hat{t} - \Sigma - \Delta)^{-1}. \quad (9)$$

To the lowest order in hybridization, we have

$$\Sigma = \Sigma^{(atom)} + G^{(atom)^{-1}} G^{(2)} G^{(atom)^{-1}} - \Delta + O(V^4). \quad (10)$$

The expansion of the Green's function in the hybridization can be done by the linked cluster expansion method following Metzner *et al.*[17] or using the auxiliary particle method[18] or by straightforward expansion of the following functional integral:

$$G_{\alpha\beta}(\tau) = \frac{\int D[f^\dagger f] f_\beta^\dagger(0) f_\alpha(\tau) \exp(-S)}{\int D[f^\dagger f] \exp(-S)}, \quad (11)$$

where

$$S = S_{local} + \sum_{\alpha\beta} \int_0^\beta d\tau \int_0^\beta d\tau' f_\alpha^\dagger(\tau) \Delta_{\alpha\beta}(\tau - \tau') f_\beta(\tau'). \quad (12)$$

Expanding to the lowest order in Δ, one obtains two first-order terms: a simple one-body term from expanding the denominator and the complicated two-body term from expanding the nominator. The correction to the atomic Green's function takes the form

$$G_{\alpha\beta}^{(2)}(i\omega) = G_{\alpha\beta}^{(atom)}(i\omega)\beta \mathrm{Tr}[G^{(atom)}\Delta] + G^2{}_{\alpha\beta}(i\omega), \quad (13)$$

where the two-particle Green's function G^2 is

$$G_{\alpha\beta}^2(i\omega) = \int_0^\beta d\tau \int_0^\beta d\tau_1 \int_0^\beta d\tau_2 e^{i\omega\tau} \times \sum_{\gamma\delta} \langle T_\tau f_\alpha(\tau) f_\beta^\dagger(0) f_\gamma^\dagger(\tau_1) f_\delta(\tau_2)\rangle_0 \Delta_{\gamma\delta}(\tau_1 - \tau_2), \quad (14)$$

and the average $\langle \cdots \rangle_0$ is the atomic average, i.e., $\mathrm{Tr}[\exp(-\beta H_{loc})\ldots]/Z$. Inserting the representation of the electron operator $f_\alpha = \Sigma_{mm'} F_{mm'}^\alpha |m\rangle\langle m'|$ in the above atomic average, one arrives at

$$\begin{aligned}
G_{\alpha\beta}^2(i\omega) &= T\sum_{i\omega'} \Delta_{\gamma\delta}(i\omega') \int d\tau \int d\tau_1 \int d\tau_2 \langle T_\tau f_\alpha(\tau) f_\gamma^\dagger(\tau_1) f_\delta(\tau_2) f_\beta^\dagger(0)\rangle e^{i\omega\tau + i\omega'(\tau_2 - \tau_1)} \\
&= \sum_{0123} \frac{e^{-\beta E_0}}{Z} T\sum_{i\omega'} \Delta_{\gamma\delta}(i\omega') \int d\tau \int d\tau_1 \int d\tau_2 [\theta(\tau > \tau_1 > \tau_2 > 0) \\
&\quad \times (F^\alpha)_{01}(F^{\gamma\dagger})_{12}(F^\delta)_{23}(F^{\beta\dagger})_{30} e^{\tau(E_0 - E_1 + i\omega) + \tau_1(E_1 - E_2 - i\omega') + \tau_2(E_2 - E_3 + i\omega')} - \theta(\tau > \tau_2 > \tau_1 > 0) \\
&\quad \times (F^\alpha)_{01}(F^\delta)_{12}(F^{\gamma\dagger})_{23}(F^{\beta\dagger})_{30} e^{\tau(E_0 - E_1 + i\omega) + \tau_2(E_1 - E_2 + i\omega') + \tau_1(E_2 - E_3 - i\omega')} - \theta(\tau_1 > \tau > \tau_2 > 0) \\
&\quad \times (F^{\gamma\dagger})_{01}(F^\alpha)_{12}(F^\delta)_{23}(F^{\beta\dagger})_{30} e^{\tau_1(E_0 - E_1 - i\omega') + \tau(E_1 - E_2 + i\omega) + \tau_2(E_2 - E_3 + i\omega')} + \theta(\tau_2 > \tau > \tau_1 > 0) \\
&\quad \times (F^\delta)_{01}(F^\alpha)_{12}(F^{\gamma\dagger})_{23}(F^{\beta\dagger})_{30} e^{\tau_2(E_0 - E_1 + i\omega') + \tau(E_1 - E_2 + i\omega) + \tau_1(E_2 - E_3 - i\omega')} + \theta(\tau_1 > \tau_2 > \tau > 0) \\
&\quad \times (F^{\gamma\dagger})_{01}(F^\delta)_{12}(F^\alpha)_{23}(F^{\beta\dagger})_{30} e^{\tau_1(E_0 - E_1 - i\omega') + \tau_2(E_1 - E_2 + i\omega') + \tau(E_2 - E_3 + i\omega)} - \theta(\tau_2 > \tau_1 > \tau > 0) \\
&\quad \times (F^\delta)_{01}(F^{\gamma\dagger})_{12}(F^\alpha)_{23}(F^{\beta\dagger})_{30} e^{\tau_2(E_0 - E_1 + i\omega') + \tau_1(E_1 - E_2 - i\omega') + \tau(E_2 - E_3 + i\omega)}].
\end{aligned} \quad (15)$$

The triple time integral can be done numerically or analytically. In the latter case, one obtains after somewhat lengthy algebra, the following expression for the two-particle Green's function in the atomic limit:

$$G^2_{\alpha\beta}(i\omega) = \sum_{0,1,2,3,\gamma\delta} (F^{\alpha})_{01}(F^{\gamma\dagger})_{12}(F^{\delta})_{23}(F^{\beta\dagger})_{30}\left[\frac{\mathcal{R}_{\gamma\delta}(E_1,E_2)}{E_{13}}\frac{1}{i\omega-E_{10}} + \frac{\mathcal{R}_{\gamma\delta}(E_3,E_2)}{E_{31}}\frac{1}{i\omega-E_{30}} + \frac{\mathcal{Q}_{\gamma\delta}(i\omega,E_0,E_2)}{(i\omega-E_{30})(i\omega-E_{10})}\right]$$
$$+ (F^{\alpha})_{01}(F^{\delta})_{12}(F^{\gamma\dagger})_{23}(F^{\beta\dagger})_{30}\left[\frac{\mathcal{R}_{\gamma\delta}(E_2,E_1)}{E_{13}}\frac{1}{i\omega-E_{10}} + \frac{\mathcal{R}_{\gamma\delta}(E_2,E_3)}{E_{31}}\frac{1}{i\omega-E_{30}} - \frac{\mathcal{Q}_{\gamma\delta}(-i\omega,E_2,E_0)}{(i\omega-E_{30})(i\omega-E_{10})}\right]$$
$$+ (F^{\gamma\dagger})_{01}(F^{\delta})_{12}(F^{\alpha})_{23}(F^{\beta\dagger})_{30}\left[\frac{\mathcal{R}_{\gamma\delta}(E_2,E_1)}{E_{20}}\frac{1}{i\omega-E_{32}} + \frac{\mathcal{R}_{\gamma\delta}(E_0,E_1)}{E_{02}}\frac{1}{i\omega-E_{30}} - \frac{\mathcal{Q}_{\gamma\delta}(-i\omega,E_3,E_1)}{(i\omega-E_{30})(i\omega-E_{32})}\right]$$
$$+ (F^{\delta})_{01}(F^{\gamma\dagger})_{12}(F^{\alpha})_{23}(F^{\beta\dagger})_{30}\left[\frac{\mathcal{R}_{\gamma\delta}(E_1,E_2)}{E_{20}}\frac{1}{i\omega-E_{32}} + \frac{\mathcal{R}_{\gamma\delta}(E_1,E_0)}{E_{02}}\frac{1}{i\omega-E_{30}} + \frac{\mathcal{Q}_{\gamma\delta}(i\omega,E_1,E_3)}{(i\omega-E_{30})(i\omega-E_{32})}\right]$$
$$+ (F^{\delta})_{01}(F^{\alpha})_{12}(F^{\gamma\dagger})_{23}(F^{\beta\dagger})_{30}\frac{1}{(i\omega-E_{21})(i\omega-E_{30})}[\mathcal{R}_{\gamma\delta}(E_2,E_3) - \mathcal{R}_{\gamma\delta}(E_1,E_0) + \mathcal{Q}_{\gamma\delta}(i\omega,E_1,E_3) - \mathcal{Q}_{\gamma\delta}(-i\omega,E_2,E_0)]$$
$$+ (F^{\gamma\dagger})_{01}(F^{\alpha})_{12}(F^{\delta})_{23}(F^{\beta\dagger})_{30}\frac{1}{(i\omega-E_{21})(i\omega-E_{30})}[\mathcal{R}_{\gamma\delta}(E_3,E_2) - \mathcal{R}_{\gamma\delta}(E_0,E_1) + \mathcal{Q}_{\gamma\delta}(i\omega,E_0,E_2) - \mathcal{Q}_{\gamma\delta}(-i\omega,E_3,E_1)], \tag{16}$$

where we used the notation $E_{ij}=E_i-E_j$ and the functions $\mathcal{R}_{\gamma\delta}$ and $\mathcal{Q}_{\gamma\delta}$ are

$$\mathcal{R}_{\gamma\delta}(E_1,E_2) \equiv (X_1+X_2)T\sum_{i\omega'}\frac{\Delta_{\gamma\delta}(i\omega')}{i\omega'-E_{12}},$$

$$\mathcal{Q}_{\gamma\delta}(i\omega,E_1,E_2) \equiv (X_1-X_2)T\sum_{i\omega'}\frac{\Delta_{\gamma\delta}(i\omega')}{i\omega'-i\omega-E_{12}}, \tag{17}$$

with the atomic probabilities given by $X_i=e^{-\beta E_i}/Z$. On the real axis these two functions take the form

$$\mathcal{R}_{\gamma\delta}(E_1,E_2) \equiv \mathrm{Re}\{X_1\Delta^-_{\gamma\delta}(E_{12}) - X_2\Delta^+_{\gamma\delta}(E_{12})\},$$

$$\mathcal{Q}_{\gamma\delta}(i\omega,E_1,E_2) \equiv X_1\Delta^-_{\gamma\delta}(i\omega+E_{12}) + X_2\Delta^+_{\gamma\delta}(i\omega+E_{12}), \tag{18}$$

where

$$\Delta^+(z) = -\frac{1}{\pi}\int\frac{f(\xi)\Delta''(\xi)d\xi}{z-\xi}, \tag{19}$$

$$\Delta^-(z) = -\frac{1}{\pi}\int\frac{f(-\xi)\Delta''(\xi)d\xi}{z-\xi}. \tag{20}$$

The constant in the first term of Eq. (13) can also be expressed by the above defined functions

$$\mathrm{Tr}[G^{(atom)}\Delta] = \sum_{0,1,\delta\gamma}(F^{\delta})_{01}(F^{\gamma\dagger})_{10}\mathcal{R}_{\gamma\delta}(E_1,E_0). \tag{21}$$

Inserting Eqs. (16), (21), (13), and (7) into Eq. (10), we finally obtain the self-energy for the impurity models requiring the impurity levels $\hat{t}$, the interaction matrix $\hat{U}$, and hybridization function $\hat{\Delta}$ as an input. Thus we find a way to calculate the exact second-order perturbation in the hybridization term. Implemented with the DMFT self-consistent condition described in Ref 1, this method can be used as a very efficient impurity solver in the DMFT study of the multiorbital systems with very complicated local interactions.

III. BENCHMARK

To test this impurity solver, we calculated the Green's function for the two-band Hubbard model at half filling and compared it with the results obtained by the QMC solver. We chose the temperature to be 0.125, where the QMC result is quite reliable. We use the semicircle density of states (DOS) and set the half bandwidth $D=1$ as the unit of energy. The metal-insulator transition has been determined by QMC at $U_c=3.5$. First let us compare the results for $U=6$, where the system is on the insulator side. We found that for a frequency higher than $\omega=U$, which is the highest energy scale in the problem, all the results obtained from three different schemes (QMC, 0th-order atomic expansion in which we simply use the atomic self-energy defined by Eq. (8), and the present solver) fall onto a single curve, which indicates that both the 0th-order atomic expansion and the present solver can capture the correct high-energy limit. For the frequency lower than U, the result obtained by the 0th-order atomic scheme shows clear deviations from the QMC data, including the second-order strong-coupling perturbation correction implemented by the present solver, and gives excellent results as shown in Fig. 1. The situation is similar for $U=4$, which is close to the Mott transition point but still on the insulator side. In this case, the deviation between the 0th-order result and the QMC result becomes quite large at low frequency, as shown in Fig. 2. For example, the relative error reaches 53% at the first Matsubara frequency. Again the error is corrected by turning on the second-order perturbation around the atomic limit in the present solver. Based on the above comparison, we can draw the conclusion that the second-order perturbation in the hybridization term works very well in the Mott insulator phase.

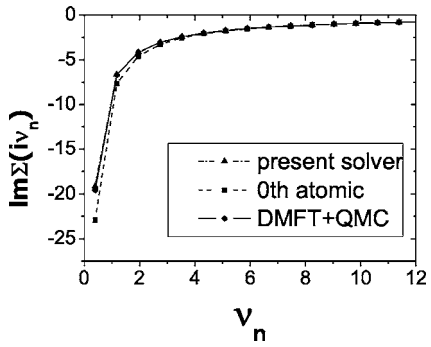

FIG. 1. The comparison of QMC and DMFT with atomic solver for the two-band Hubbard model with $U=6$, $\mu=0$, $T=0.125$, and half bandwidth $D=1$.

Another good test for this impurity solver is the antiferromagnetic (AF) order in the half-filled single-band Hubbard model on a bipartite lattice. In the large U limit, it is well known that in such a case up to the second-order perturbation in t/U, the Hubbard model can be mapped to an antiferromagnetic Heisenberg model with exchange energy $J \propto t^2/U$. Since the exchange energy is the only energy scale in the problem, the Neel temperature must also be proportional to $1/U$ in large U limit. Although the physics behind this is quite straightforward, it is not reproduced by equation of motion (EOM) or IPT methods within the framework of DMFT. Although the Hartree-Fock approximation can also obtain the correct AF order in the ground state, it predicts the Neel temperature to be of order U instead of J, as shown in Fig. 3. Since the impurity solver we propose here can include exactly the second-order correction to the atomic limit, we expect that it can reproduce the correct Neel temperature in the large U limit. For this purpose, we solved the single-band Hubbard model at half filling on the unfrustrated Bethe lattice and compared the results with the Hartree-Fock approximation, DMFT+IPT and DMFT+QMC in Fig. 3. Since the self-energy obtained by the present impurity solver vanishes when $U=0$, we can also get the correct result for the noninteracting case. That is why the Neel temperature obtained by the present solver goes down in the small U limit. A very good agreement between our results and the QMC results is found for $U/D > U_c$, where $U_c=3.5$ is approximately the U_{c2}

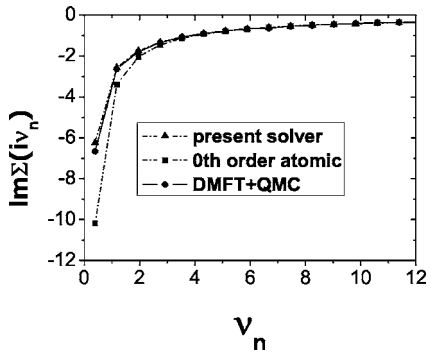

FIG. 2. The comparison of QMC and DMFT with the atomic solver for the two-band Hubbard model with $U=4$, $\mu=0$, $T=0.125$ and half bandwidth $D=1$.

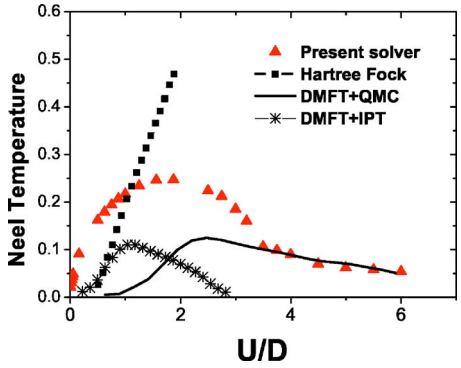

FIG. 3. (Color online) The comparison of the Neel temperature obtained by QMC, IPT, Hatree-Fock, and the atomic solver for a half-filled single-band Hubbard model with half bandwidth $D=1$.

in the Mott transition in the paramagnetic phase.[19] We also show the results obtained by iterative perturbation theory and Hartree-Fock approximation in Fig. 3, which are far away from the QMC results for almost the whole range of U. The remarkably good agreement between our results and the QMC data in the large U limit indicates that combined with LDA, this simple impurity solver can be used to carry out the first-principles calculation of the ordering temperature of the materials which have spin-orbital long-range order in the ground states in the framework of LDA+DMFT. Compared with the model Hamiltonian studies, in which the superexchange processes are considered by the Heisenberg model, the LDA+DMFT approach has two advantages. The first one is that unlike the Heisenberg model, which can only capture the low-energy physics, the LDA+DMFT can capture not only the low-energy physics like the long-range spin-orbital order but also the high-energy physics like the Hubbard bands. Besides that, since the effective bath in DMFT does not come only from the nearest-neighbor sites, the LDA+DMFT calculation can include the long-range coupling between the local spins in a natural way.

For the paramagnetic phase of a SU(N) Anderson impurity model, the self-energy of the present solver is simple enough to be written as a closet expression. It becomes particularly simple in the case of half filling where it takes the form

$$\Sigma(z) = \left(\frac{U}{2}\right)^2 \frac{1}{z}\left(1 + \frac{3\Delta(z)}{z}\right). \tag{22}$$

To get the DMFT solution, we also need the DMFT self-consistency condition. For the Bethe lattice, it is simply given by $\Delta = t^2 G$, therefore the DMFT local Green's function takes the form

$$G_{DMFT}(z) = \frac{1}{2\tau(z)^2}[x - s\sqrt{x^2 - 4\tau(z)^2}], \tag{23}$$

where $\tau(z) = t\sqrt{1+\frac{3}{4}(U^2/z^2)}$, $x=(z-U/2)(z+U/2)/z$, and $s = \sin\{\mathrm{Im}[x^2-4\tau(z)^2]\}$.

The spectral function that corresponds to Eq. (23) is plotted in Fig. 4 for various values of U, ranging from $U=0$ to $U=6$. For comparison, we also displayed the NRG results at

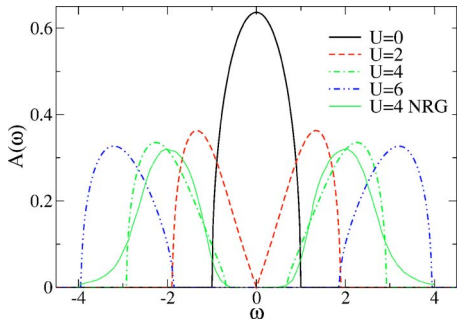

FIG. 4. (Color online) The spectral function of the one-band Hubbard model on the Bethe lattice for various values of U compared with the NRG results (taken from Ref. 20).

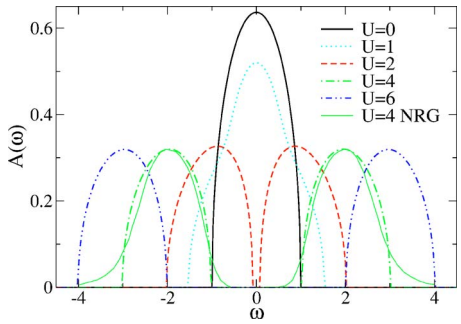

FIG. 5. (Color online) The DMFT spectral function obtained by using self-energy from Eq. (24) compared with the NRG results.

$U=4$. It is clear that the present solver misses the Kondo effect and therefore should be used only in the insulating state, i.e., when the spectral function has a finite gap. At $U=4$ we can see that the width of the gap as well as the position of the Hubbard bands is very close to the NRG results. Note, however, that the NRG has a finite resolution at high frequencies and therefore does not provide very precise Hubbard bands either. They usually tend to be slightly rounded.

It is well known that deep in the insulating state, the width of the Hubbard bands as well as the shape of the Hubbard bands has to be the same as the noninteracting density of states. As one can see in Fig. 4, the width is indeed $2D$ and they become more and more semicircular as U increases. Note that the zeroth-order approximation [expressed by Eq. (8)] gives a factor of 2 narrower Hubbard bands. Finally, the critical U, at which the gap closes, is $2\sqrt{3}$ and is reasonably close to the exact upper critical U being $U_{c2} \sim 2.97$.

It should be noted that the perturbation theory in the hybridization is a singular perturbation for the metallic system, therefore any finite-order perturbation cannot offer a qualitatively proper description of the system. If one does apply the present solver to the metallic system, the local Green's function develops a pole in the complex plane which does not lie on the real axis. This pole indicates a tendency toward the formation of a singularity at the Fermi level. Namely, some weight is missing under the Hubbard bands and the spectral function develops a V-shaped cusp at the Fermi level.

To avoid the causality problem in the metallic state, one might rewrite the self-energy in the continued fraction representation which has the same lowest-order term in expansion in Δ. For the half-filled one-band model, the following self-energy can be constructed in this way:

$$\Sigma(z) = \left(\frac{U}{2}\right)^2 \frac{1}{z - 3\Delta(z)}. \tag{24}$$

The DMFT spectral function that corresponds to this self-energy is plotted in Fig. 5. In this approximation, the system is metallic for $U < \sqrt{3}$; however, the metallic state is not Fermi liquid and therefore the spectral function does not reach the unitary limit at $\omega=0$. However, the causality problem is avoided and the impurity solver does not break down in the metallic state. The agreement in position and shape of the Hubbard bands is also improved in the insulating state of the system. Note almost perfect agreement between NRG and the present solver spectral function at $U=4$. As an efficient impurity solver in the strong-coupling limit, the present solver should be compared with two other impurity solvers, which are commonly used in this limit, namely the equation of motion method[11] (EOM) and NCA.[9] Unlike the method proposed in this paper, the EOM method requires a self-consistent procedure to obtain the Green's function on the impurity site. A general impurity model generated by LDA+DMFT usually contains a large number of orbits and very complicated non-SU(N)-like local interaction. Therefore in the EOM method one has to solve the self-consistent equations with very large number of parameters, which is almost impossible numerically when the orbital number reaches 14 as in systems with one open f shell per unit cell. The NCA method suffers from the same problem when the orbital number becomes large and the system is away from the SU(N) symmetry since the number of atomic states, and therefore pseudoparticles, grows exponentially. Compared with other impurity solvers, the main advantage of the present solver is that no self-consistent loop is required to solve the impurity problem and the local interaction can be very general, including local Coulomb repulsion, Hunds coupling, spin-orbital coupling, and pair-hopping term. The computational time of the present impurity solver still grows as N^4, where N is the number of atomic states, since one needs to carry out four sums in Eq. (16). Note, however, that the matrix $F^{\alpha}_{nn'}$ has many zero elements and if one takes into account the conservation of spin and particle number, the computational time can be considerably reduced. At present, for a general f system, it takes only a few seconds on modern computers.

IV. CONCLUSIONS

To summarize, this paper presents a new impurity solver based on second-order perturbation theory in the hybridization around the atomic limit. The strength of the approach lies in its generality and its speed. It can be applied to systems with very complicated atomic configurations, general Coulomb repulsion, and spin-orbit coupling and does not require self-consistency therefore it can be efficiently applied to a system with open d or f shells. It is, however, limited to

integer filling and large U, which is the regime particularly important for studying transition-metal compounds in the Mott insulating state with or without orbital or magnetic long-range order.

ACKNOWLEDGMENT

This work was supported by the NSF under Grant No. DMR-0096462.

*Electronic address: daix@hkucc.hku.hk

[1] A. Georges, G. Kotliar, W. Krauth, and M. J. Rozenberg, Rev. Mod. Phys. **68**, 13 (1996).

[2] V. Anisimov, A. Poteryaev, M. Korotin, A. Anokhin, and G. Kotliar, J. Phys.: Condens. Matter **9**, 7359 (1997); K. Held, I. A. Nekrasov, G. Keller, V. Eyert, N. Blümer, A. K. McMahan, R. T. Scalettar, Th. Pruschke, V. I. Anisimov, and D. Vollhardt, Psi-k Newsletter No. 56 (April 2003), p. 65; A. I. Lichtenstein, M. I. Katsnelson, and G. Kotliar, in *Electron Correlations and Materials Properties 2* edited by A. Gonis, N. Kioussis, and M. Ciftan (Kluwer, New York, 2003).

[3] A. I. Lichtenstein and M. I. Katsnelson, Phys. Rev. B **57**, 6884 (1998).

[4] S. Biermann, F. Aryasetiawan, and A. Georges, Phys. Rev. Lett. **90**, 086402 (2003).

[5] X. Dai, S. Y. Savrasov, G. Kotliar, A. Migliori, H. Ledbetter, and E. Abrahams, Science **300**, 953 (2003); S. Y. Savrasov, G. Kotliar, and E. Abrahams, Nature (London) **410**, 793 (2001).

[6] K. Held, G. Keller, V. Eyert, D. Vollhardt, and V. I. Anisimov, Phys. Rev. Lett. **86**, 5345 (2001).

[7] M. J. Rozenberg, G. Kotliar, and X. Y. Zhang, Phys. Rev. B **49**, 10181 (1994).

[8] S. Y. Savrasov, V. Oudovenko, K. Haule, D. Villani, and G. Kotliar, Phys. Rev. B **71**, 115117 (2005).

[9] M. Jarrell, and Th. Pruschke, Phys. Rev. B **49**, 1458 (1994); K. Haule, V. Oudovenko, S. Y. Savrasov, and G. Kotliar, Phys. Rev. Lett. **94**, 036401 (2005).

[10] G. Kotliar and A. E. Ruckenstein, Phys. Rev. Lett. **57**, 1362 (1986).

[11] H. O. Jeschke and G. Kotliar, Phys. Rev. B **71**, 085103 (2005); Jian-Xin Zhu, R. C. Albers, J. M. Wills, cond-mat/0409215 (unpublished).

[12] M. Capone, M. Fabrizio, C. Castellani, and E. Tosatti, Phys. Rev. Lett. **93**, 047001 (2004); A. Koga, N. Kawakami, T. M. Rice, and M. Sigrist, *ibid.* **92**, 216402 (2004).

[13] L. Laloux, A. Georges, and W. Krauth, Phys. Rev. B **50**, 3092 (1994).

[14] L. Chioncel, L. Vitos, I. A. Abrikosov, J. Kollar, M. I. Katsnelson, and A. I. Lichtenstein, Phys. Rev. B **67**, 235106 (2003); V. Drchal, V. Janiš, J. Kudrnovsky, V. S. Oudovenko, X. Dai, K. Haule, and G. Kotliar, J. Phys.: Condens. Matter **17**, 61 (2005).

[15] Y. Tokura and N. Nagaosa, Science **288**, 462 (2000).

[16] E. Pavarini, S. Biermann, A. Poteryaev, A. I. Lichtenstein, A. Georges, and O. K. Andersen, Phys. Rev. Lett. **92**, 176403 (2004).

[17] W. Metzner, Phys. Rev. B **43**, 8549 (1991); T. D. Stanescu and G. Kotliar, *ibid.* **70**, 205112 (2004).

[18] K. Haule, S. Kirchner, J. Kroha, and P. Wölfle, Phys. Rev. B **64**, 155111 (2001).

[19] A. Georges and W. Krauth, Phys. Rev. B **48**, 7167 (1993); M. J. Rozenberg, G. Kotliar, and X. Y. Zhang, *ibid.* **49**, 10181 (1994).

[20] R. Bulla, cond-mat/0412314 (unpublished).